RESEARCH ARTICLE

Functional Ecology | BRITISH ECOLOGICAL SOCIETY

Age-prevalence curves in a multi-species parasite community

Daniel L. Preston[1,2] 🔅 | **Landon P. Falke**[3] | **Mark Novak**[4]

[1]Department of Fish, Wildlife, and Conservation Biology, Colorado State University, Fort Collins, Colorado, USA

[2]Graduate Degree Program in Ecology, Colorado State University, Fort Collins, Colorado, USA

[3]Integrated Statistics Contractor for the National Oceanic and Atmospheric Administration, Northeast Fisheries Science Center, Woods Hole, Massachusetts, USA

[4]Department of Integrative Biology, Oregon State University, Corvallis, Oregon, USA

Correspondence
Daniel L. Preston
Email: dan.preston@colostate.edu

Handling Editor: Amy Pedersen

Abstract

1. The relationship between infection prevalence and host age is informative because it can reveal processes underlying disease dynamics. Most prior work has assumed that age-prevalence curves are shaped by infection rates, host immunity and/or infection-induced mortality. Interactions between parasites within a host have largely been overlooked as a source of variation in age-prevalence curves.

2. We used field survey data and models to examine the role of interspecific interactions between parasites in shaping age-prevalence curves. The empirical dataset included quantification of parasite infection prevalence for eight co-occurring trematodes in over 15,000 snail hosts. We characterized age-prevalence curves for each taxon, examined how they changed over space in relation to co-occurring trematodes and tested whether the shape of the curves aligned with expectations for the frequencies of coinfections by two taxa in the same host. The models explored scenarios that included negative interspecific interactions between parasites, variation in the force-of-infection (FOI) and infection-induced mortality that varied with host age, which were mechanisms hypothesized to be important in the empirical dataset.

3. In the empirical dataset, four trematode parasites had monotonic increasing age-prevalence curves and four had unimodal age-prevalence curves. Some of the curves remained consistent in shape in relation to the prevalence of other potentially interacting trematodes, while some shifted from unimodal to monotonic increasing, suggesting release from negative interspecific interactions. The most common taxa with monotonic increasing curves had lower co-infection frequencies than expected, suggesting they were competitively dominant. Taxa with unimodal curves had coinfection frequencies that were closer to those expected by chance.

4. The model showed that negative interspecific interactions between parasites can cause a unimodal age-prevalence curve in the subordinate taxon. Increases in the FOI and/or infection-induced mortality of the dominant taxon cause shifts in the peak prevalence of the subordinate taxon to a younger host age. Infection-induced mortality that increased with host age was the only scenario that caused a unimodal curve in the dominant taxon.

5. Results indicated that negative interspecific interactions between parasites contributed to variation in the shape of age-prevalence curves across parasite taxa and support the growing importance of incorporating interactions between parasites in explaining population-level patterns of host infection over space and time.

1 | INTRODUCTION

While many studies on wildlife disease have focused on interactions between a single-host and a single-parasite taxon, virtually all hosts in nature support a diverse community of infectious agents (Petney & Andrews, 1998). In some cases, infection by multiple parasites may worsen disease for hosts in an additive manner, reducing host fitness (Johnson & Hoverman, 2012). In other cases, parasites interact with one another in complex ways, including directly (e.g. via competition for space or food), or indirectly (e.g. via interactions with the host immune system) (Cattadori et al., 2008; Ezenwa, 2016; Viney & Graham, 2013). These mechanisms can result in negative interspecific interactions or in some cases, facilitation (Halliday et al., 2020). BInteractions between co-infecting parasites can influence the dynamics of the host and parasite populations (Fenton, 2008; Marchetto & Power, 2018; Susi et al., 2015), as well as patterns of parasite community structure (Halliday et al., 2020; Karvonen et al., 2019; Pedersen & Fenton, 2007; Rynkiewicz et al., 2015). Despite the growing recognition of the ecological importance of parasite interactions, detecting and interpreting the underlying mechanisms that drive observed patterns remains a significant challenge.

One useful approach for inferring disease processes from observational data is the use of age-prevalence (or age-intensity) curves. The force-of-infection (FOI) (i.e. the per-host rate of acquiring an infection) is a key component of transmission models and can be estimated in some cases from age-prevalence data (Caley et al., 2009; McCallum et al., 2001). The basic assumption that host age reflects exposure duration spurred the development of 'catalytic models' for estimating FOI and how it can vary over space and time due to ecological factors or disease interventions (Cohen, 1973; Hairston, 1965; Muench, 1959). In a straightforward situation with a constant FOI and a relatively homogeneous host population, infection prevalence can be expected to increase with host age because older individuals have a longer time period of exposure to parasites (Heisey et al., 2006). This pattern has been observed in a range of host–parasite systems, including schistosome worms in freshwater snails (Graham, 2003), trypanosomes in tsetse flies (Woolhouse et al., 1994) and tapeworms in sheep (Dueger & Gilman, 2001).

In many cases, however, age-prevalence curves diverge from expectations based on a constant FOI and homogenous host population. Factors including variation in parasite exposure, host resistance to infection and host mortality can affect the shape of age-prevalence curves (Caley & Hone, 2002; Heisey et al., 2006; Woolhouse, 1998). For instance, the FOI may be higher in younger, intermediate or older hosts due to an ability of free-living infectious stages to 'choose' their host (Horn et al., 2023; Theron & Rognon, 1998; Wunderlich et al., 2022) or from passive differences in exposure correlated with host body size (Poulin, 2000). Host mortality from infection can also drive variation in age-prevalence curves, for instance by eliminating older infected individuals from the population and lowering the plateau of the curve (Heisey et al., 2006). Additionally, increased parasite clearance by older/larger size classes (e.g. from adaptive immunity gained by an individual over time) can drive a decrease in prevalence of older hosts, creating a unimodal age-prevalence curve (sometimes called 'convex' in the disease ecology literature) (Anderson & May, 1979, 1985; Woolhouse, 1998). Determining which of these non-mutually exclusive processes generate an observed age-prevalence curve in observational data from a wild host population is challenging.

Infection prevalence patterns can also be affected by interactions between parasites. For example, digenetic trematodes infecting snails can exhibit antagonistic interactions between one another via direct predation or the secretion of toxic chemicals (Hechinger et al., 2011; Heyneman & Umathevy, 1968; Lafferty, 2002; Lie, 1973; Lim & Heyneman, 1972). Antagonistic interactions between parasites can make dominant parasites more common in older hosts and competitively inferior parasites more common in younger hosts, potentially leading to distinct age-prevalence curves across parasite taxa within the same community (Kuris, 1990). Most prior empirical and modelling studies on age-prevalence curves, however, have omitted the potentially important role of parasite interactions in driving observed patterns. This gap stems in part from a lack of age-prevalence data on species-rich parasite communities that are well-replicated across host populations. Replicated age-prevalence curves can be used to test whether the curve is sensitive to hypothesized factors that may change over space, such as the abundance of interacting parasite taxa or environmental variables (Woolhouse, 1998). Several modelling and empirical studies have examined effects of parasite–parasite interactions on age-intensity curves of macroparasites (see Bottomley et al., 2005; Duerr et al., 2003; Park & Ezenwa, 2020); however, for parasites that multiply within their host it may be challenging to detect effects of interspecific parasite interactions on infection intensity. In these cases, characterizing age-prevalence curves may provide a useful alternative approach that can be applied to cross-sectional field data.

Our overall objective was to evaluate support for hypothesized mechanisms underlying observed age-prevalence curves in a multi-species parasite community. We focused on a community of digenetic trematodes infecting stream snails that had potential to show wide variation in the shape of their age-prevalence curves across taxa. Our null hypothesis was that in the absence of more complex mechanisms, age-prevalence curves would be monotonically increasing due to increased exposure times with increasing host age, a pattern commonly observed in snail–trematode interactions (Graham, 2003; Sorensen & Minchella, 2001). In contrast, if age-prevalence curves were unimodal, we hypothesized that two types of mechanisms could be important: (1) factors that are intrinsic to the focal pairwise host–parasite interaction, namely infection-induced mortality and/or clearance of infections over time (Anderson & May, 1979; Cohen, 1973; Esch & Fernandez, 1994), or (2) direct negative interactions between parasites, which could result in the loss of competitively inferior taxa in older/larger host individuals (Heyneman & Umathevy, 1968; Kuris, 1990; Lie, 1973; Lim & Heyneman, 1972).

We used a combination of empirical data and models to evaluate support for these different processes. The empirical dataset involved over 15,000 host dissections, which we used to describe variation in the shape of age-prevalence curves across parasite taxa and in relation to potentially interacting heterospecific trematodes. We predicted that if parasite interactions were important in driving the observed age-prevalence curve then the shape of the curve for competitively inferior taxa would change from unimodal to monotonic with a decrease in the FOI of competitively dominant trematodes. Alternatively, if factors intrinsic to the focal host–parasite interactions (e.g. acquired immunity or infection-induced mortality) were more important, we predicted that the overall shape of age-prevalence curves would be relatively invariant over the spatial scale of our study (one watershed). We additionally quantified the occurrence of co-infected hosts with multiple trematode taxa and evaluated whether co-infection patterns aligned with hypotheses explaining variation in the shape of age-prevalence curves. We predicted that competitively inferior taxa (which we expected to have unimodal age-prevalence curves) would be more common in coinfections than competitively dominant taxa (which were expected to have monotonic increasing age-prevalence curves). Finally, to help explain the possible mechanisms underlying the observed patterns in the field data—and to extend the generality of our study—we also used simple models to explore how changes in the FOI, host mortality and parasite–parasite interactions changed the shape of hypothetical age-prevalence curves.

2 | METHODS

2.1 | Study system

We characterized age-prevalence curves of trematodes infecting freshwater stream snails (*Juga plicifera*) in Oregon, USA. *J. plicifera* is a relatively large (up to 30 mm), long-lived (up to 7 years) and locally abundant freshwater snail that inhabits streams and rivers in the Pacific Northwest (Campbell et al., 2016; Hawkins & Furnish, 1987; Strong & Whelan, 2019). *J. plicifera* are first intermediate hosts to a diverse guild of trematode parasites that have multi-host life cycles, usually including a vertebrate definitive host (Falke & Preston, 2022; Pratt & McCauley, 1961; Preston et al., 2021). Definitive hosts deposit trematode eggs into the stream, which hatch into infectious stages that infect snails. The numbers of trematode eggs deposited in the aquatic environment is a determinant of the FOI experienced by host snails and can thus vary over space and time due to definitive host abundance and space use (Byers et al., 2015; Smith, 2001).

2.2 | Empirical age-prevalence curves

In summer of 2019 and 2020, we surveyed *Juga* snails and their trematodes at 137 stream sites in the Willamette River Basin in western Oregon (see Appendix S1, Figure S1 for a study area map). Twenty-five of the sites were on the mainstem Willamette River and 18 to 20 sites were within each of six major tributaries (Appendix S1, Figure S1). Survey sites ranged from first to eighth order streams and varied in local environmental factors including discharge volume, gradient, riparian vegetation and surrounding land cover (Falke & Preston, 2021). At each site, we collected approximately 100 *Juga* snails (mean = 111) for parasite quantification, resulting in a total of 15,190 host snails dissected. All snails were measured for total shell length (mm), crushed gently with pliers and then examined under a dissecting microscope (8×–35× magnification) for the presence of trematode larvae. Wet mounts were examined under a compound microscope (40×–1000× magnification) to aid in identifying immature infections. Trematodes were initially identified based on comparisons of morphotypes to previously described species infecting the same host snails in the same geographic area (Bennington & Pratt, 1960; Burns, 1961; Burns & Pratt, 1953; McCauley & Pratt, 1961; Meade & Pratt, 1965; Pratt & McCauley, 1961). We then used data obtained from molecular sequencing of nuclear 28S rDNA to further identify trematodes, most to genus or species (see Falke & Preston, 2022; Preston et al., 2021 for additional details). Field data were conducted under Oregon Department of Fish and Wildlife permit #26611. This study did not require an Animal Care and Use Committee protocol because vertebrates were not involved.

To first visualize age-prevalence curves for each trematode taxon, we calculated the proportion of infected snails for eight host size classes, ranging from <12.5 to >27.5 mm. Host snails <10 mm were not dissected in surveys due the rarity of infections below that size, and thus the smallest size class was individuals between 10 and 12.5 mm. For each size class, we calculated 95% binomial confidence intervals using the Wilson score method (Wilson, 1927). Extremely rare trematode taxa (<1% total prevalence) were excluded, resulting in curves for eight taxa. *Juga* snails have indeterminate growth, although growth rates decrease with increasing age (Diamond, 1982). We explored converting host size to host age using previously developed growth rate functions, but

decided against this due to expected variation in growth rates across survey sites (e.g. due to temperature and other environmental factors). We therefore used host body size as a proxy for host age. We first characterized age-prevalence curves across taxa using infection data from all 137 sites combined. These curves therefore incorporated a variety of ecological processes over space, including variation in parasite recruitment and possible interspecific interactions between trematodes.

We next used generalized additive models (GAMs) with a binomial response (infected or uninfected) to characterize the relationships between host size, possible interspecific interactions and individual host infection probability. We first ran a model for all taxa combined (infection by any trematode) and separate models for each trematode taxon individually ($n = 8$ taxa) with only a smoothing term for host size. Next, to assess the possible role of interspecific interactions, we included an interaction between host size and a categorical variable (high/low) representing the prevalence of four trematode taxa that we hypothesized were sufficiently abundant to have a detectable effect on the shape of the age-prevalence curves of other taxa. These four taxa were *Acanthatrium oregonense*, *Metagonimus* sp., *Nanophyetus salmincola* and *Metagonimoides oregonensis* (see Figure 2 for their infection prevalences). We calculated the median site-level infection prevalence of these four taxa and then divided the full dataset (all 137 sites) into two subsets for each taxon: sites with a prevalence above or below the median for each of these four taxa. We used this categorical variable as the predictor in the models including interspecific interactions. We ran separate models for each interacting trematode pair and compared the relative performance of the models with and without the interactions using Akaike information criterion (AIC) (Burnham & Anderson, 2003). GAMs were fit with the 'mgcv' package with the default levels of smoothing (Wood, 2017). To visualize the GAM results in relation to age-prevalence curves, we generated partial effects plots showing infection probabilities in relation to host size for each model. Prior to analyses, we examined whether the prevalences of these four trematodes were correlated with one another at the site-level using Pearson correlation coefficients (maximum $r = 0.23$, Appendix S1, Figure S2). We hypothesized that unimodal curves of a subordinate parasite would shift to monotonic increasing at low prevalences of a dominant parasite within a pair; alternatively, if interspecific interactions were unimportant, we expected the curves to remain relatively consistent in shape in relation to the prevalence of potentially interacting taxa.

2.3 | Coinfections

To further evaluate whether interspecific interactions between parasites were affecting size-prevalence curves, we quantified the numbers of co-infections by more than one trematode in a single host and compared this to values expected by random chance using a Fisher's exact test (Agresti, 2012) with p-values estimated via a Monte Carlo method using the 'stats' package (R Core Team, 2023). If negative interspecific interactions were occurring, we expected coinfections to be rarer than expected by chance for a given pair, which in turn was hypothesized to generate unimodal age-prevalence curves in the competitively inferior taxon. To account for heterogeneity in trematode colonization to snails across survey sites, we only included sites where both taxa in each pair were observed infecting at least one host snail each. This approach avoided confounding a lack of recruitment with negative interspecific interactions and resulted in a mean of 37 sites per taxon combination. In addition to the survey data described above, we also included dissection data from three previously surveyed sites in the same region where an additional 3851 snails were dissected (Falke & Preston, 2022). At each of these three sites, we dissected snails collected from within $0.5\,m^2$ quadrats placed every meter along a $50\,m$ reach (i.e. 50 total quadrats). Snails were measured and dissected as describe above. This increased the number of observed co-infections, allowing stronger inferences about trematode-trematode interactions. To calculate expected frequencies of coinfections, we calculated the product of the observed infection prevalences of the two taxa in each pairwise combination at each site (Kuris, 1990). This approach resulted in conservative estimates of expected co-infection frequencies, but does not require assuming an a priori hierarchy of competitive interactions.

2.4 | Age-prevalence models

We used two different modelling approaches to address how the hypothesized processes affect the shape of age-prevalence curves. In the first approach, we used ordinary differential equations (ODEs) to generate age-prevalence curves by assuming that time and host age are synonymous. Following Anderson & May (1979), this approach tracked a single cohort of host individuals that start out uninfected at birth and become infected or die over time. In the second approach, we used partial differential equations (PDEs) to treat time and age distinctly and incorporated both host mortality and reproduction, allowing us to assess changes in the shape of the age-prevalence curves over time. The long-term steady state age-prevalence curves generated by the PDEs were equivalent to those generated by the ODEs; we thus focus on the ODEs in the main text and the PDEs in Appendix S2.

The models involved two parasite species sharing the same host population. The equations tracked uninfected hosts, hosts infected with a dominant parasite and hosts infected with a subordinate parasite. Hosts infected with the subordinate parasite could become infected by the dominant parasite, but hosts infected by the dominant parasite could not become infected by the subordinate parasite. Uninfected hosts could be infected by either parasite. To generate age-prevalence curves, we calculated the proportion of

hosts infected with each parasite as the cohort ages. The equations were as follows:

$$\frac{dx}{dt} = -\lambda_y x - \lambda_z x,$$

$$\frac{dy}{dt} = \lambda_y x + \lambda_y z - u_y,$$

$$\frac{dz}{dt} = \lambda_z x - \lambda_y z - u_z,$$

where dx/dt is the rate of change of uninfected hosts, dy/dt is the rate of change of hosts infected with the dominant parasite, and dz/dt is the rate of change of hosts infected with the subordinate parasite. The FOI for the dominant parasite (λ_y) and the subordinate parasite (λ_z), and the infection-induced mortality rate for the dominant parasite (μ_y) and the subordinate parasite (μ_z), were represented as either constant values over time or as functions changing with host age. We explored four scenarios hypothesized to drive variation in the shape of age-prevalence curves: (1) a difference in the FOI between dominant and subordinate parasite, (2) variation in FOI over host age, (3) a difference in infection-induced mortality between dominant and subordinate parasite and (4) variation in infection-induced mortality over host age. Specific parameter values are provided in Table 1. The model was implemented using the 'deSolve' function in R (R Core Team, 2023; Soetaert et al., 2010).

3 | RESULTS

3.1 | Empirical age-prevalence curves

For all trematode taxa combined, the age-prevalence curve was monotonic and increased to 94% infection prevalence in snails >27.5 mm (Figure 1a). For all taxa combined, and for seven of eight individual taxa, host size was related to infection probability (GAMs, all $p < 0.001$, Appendix S1, Table S1). For one taxon that was relatively rare (*P. siliculus*), host size was not as clearly related to infection probability (GAM, $p = 0.05$). Curves for three trematode taxa generally increased with host size (Figure 1b,c,f) and curves for four taxa were unimodal, with peak prevalence varying from 15 to 27 mm across taxa (Figure 1d,e,h,i). One curve was approximately linear (*N. salmincola*; GAM: effective degrees of freedom = 1), two were somewhat non-linear (*C. alseae* and *D. aspina*; edf = 1 to 2); and the rest were strongly nonlinear (edf > 2; Appendix S1, Table S1).

Including an interaction between focal host size and the prevalence of the four most abundant trematodes generally improved relative model performance (i.e. lowered AIC; Appendix S1, Table S2); however, the degree to which curve shape was influenced by the consideration of abundant taxa varied by focal taxon (see Figure 2; Appendix S1, Figures S3–S6 for partial effects plots showing relationships between host size and infection probability). One taxon, *M. oregonensis*, had an infection probability that always increased with host age regardless of the prevalence of the other three most abundant taxa (Figure 2a–d). *Nanophyetus salmincola* also had a relatively consistent monotonic increasing infection probability in relation to prevalence of two other taxa (*M. oregonensis* and *A. oregonense*) but showed some variation in relation to the prevalence of *Metagonimus* sp. (Figure 2e–h; Appendix S1, Table S2). For *Metagonimus* sp., infection probability increased at low prevalences of the other three abundant trematode taxa (*A. oregonense*, *N. salmincola*, *M. oregonensis*) and became unimodal when those taxa were at high prevalence (Figure 2i–l). *Acanthatrium oregonense* showed the same pattern in relation to infection prevalence of *N. salmincola* (Figure 2n). The relationship between prevalence and host size of the other four non-abundant taxa was less sensitive to coinfection, with model performance little changed by incorporating interspecific interactions (Appendix S1, Figures S3–S6, Table S2).
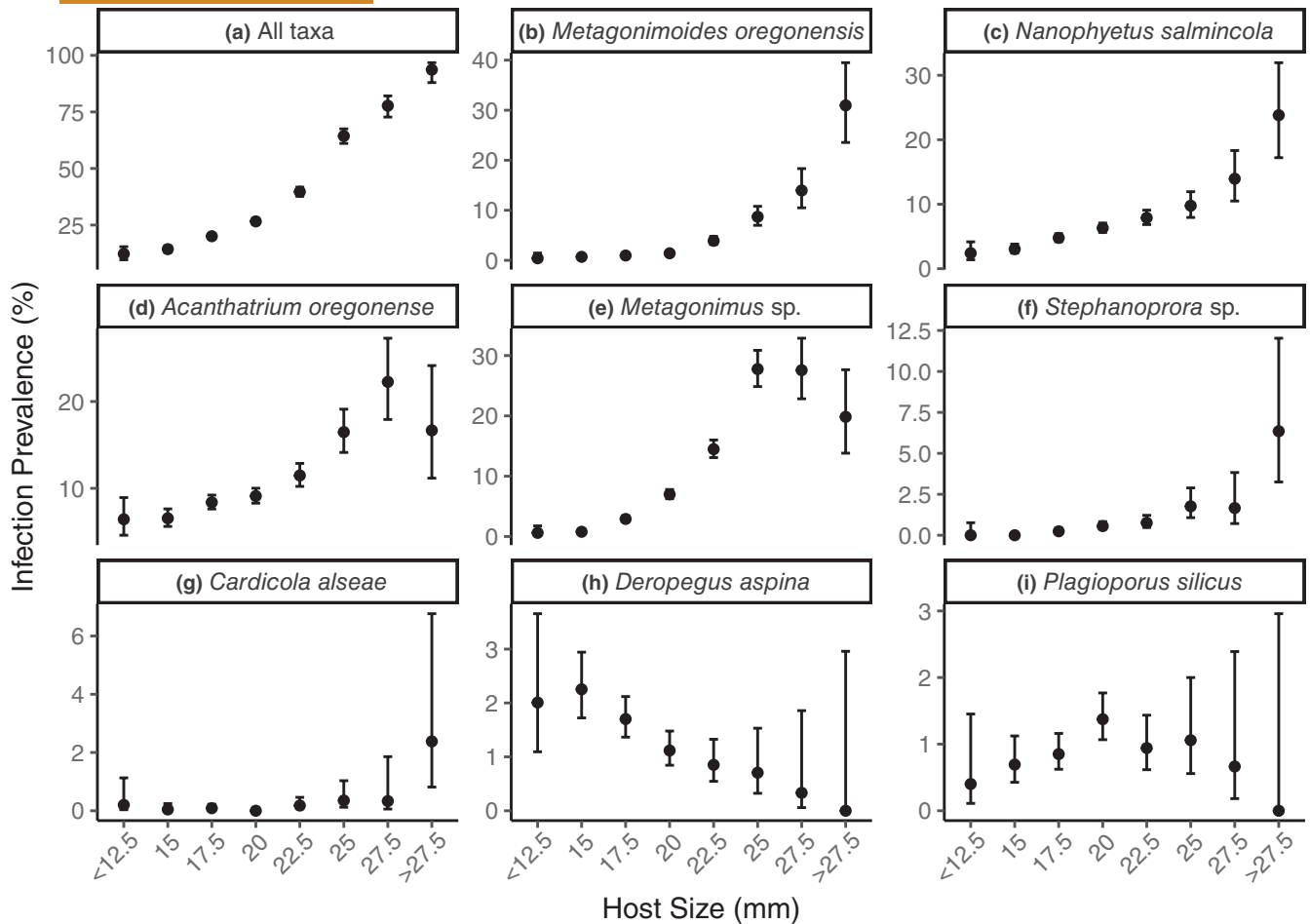
TABLE 1 Parameter values for age-prevalence models. The four scenarios ('a' through 'd' in the table) correspond to the four panels in Figure 1. Each row within a scenario represents a separate model run with the colour in parentheses corresponding to those used in Figure 1. Parameter definitions are as follow: λ_y is the force-of-infection for the dominant parasite, λ_z is force-of-infection for the subordinate parasite, μ_y is the infection-induced mortality for the dominant parasite, and μ_z is the infection-induced mortality for the subordinate parasite.

Scenario	Parameters
(a) FOI varies between parasites	
(1) Equal FOI	$\lambda_y=0.01$, $\lambda_z=0.01$, $\mu_y=0.01$, $\mu_z=0.01$ (purple)
(2) FOI higher for subordinate	$\lambda_y=0.005$, $\lambda_z=0.02$, $\mu_y=0.01$, $\mu_z=0.01$ (teal)
(3) FOI higher for dominant	$\lambda_y=0.02$, $\lambda_z=0.005$, $\mu_y=0.01$, $\mu_z=0.01$ (yellow)
(b) FOI varies with host age and between parasites	
(1) FOI increases with age for dominant	$\lambda_y=0.001$ (age), $\lambda_z=0.01$, $\mu_y=0.01$, $\mu_z=0.01$ (teal)
(2) FOI increases with age for subordinate	$\lambda_y=0.01$, $\lambda_z=0.001$ (age), $\mu_y=0.01$, $\mu_z=0.01$ (yellow)
(c) Infection-induced mortality varies between parasites	
(1) Mortality higher for dominant	$\lambda_y=0.01$, $\lambda_z=0.01$, $\mu_y=0.05$, $\mu_z=0.02$ (teal)
(2) Mortality higher for subordinate	$\lambda_y=0.01$, $\lambda_z=0.01$, $\mu_y=0.02$, $\mu_z=0.05$ (yellow)
(d) Infection-induced mortality varies with host age and between parasites	
(1) Mortality increases with age for dominant	$\lambda_y=0.01$, $\lambda_z=0.01$, $\mu_y=0.1$ $(1-\exp^{-0.02(age)})$, $\mu_z=0.01$ (teal)
(2) Mortality decreases with age for dominant	$\lambda_y=0.01$, $\lambda_z=0.01$, $\mu_y=0.1$ $(\exp^{-0.02(age)})$, $\mu_z=0.01$ (yellow)

FIGURE 1 Age-prevalence data for (a) all taxa combined and (b–i) the eight trematodes individually. Infection prevalence values are shown with 95% binomial confidence intervals calculated using the Wilson score method. Data are from dissections of 15,190 host snails. Note the differences in the *y*-axis scale across panels. The labels on the *x*-axis indicate the upper end of the size bin. Curves include the following numbers of dissected snails per size bin: 10 to 12.5 mm (498), 12.5 to 15 mm (2308), 15 to 17.5 mm (4583), 17.5 to 20 mm (4293), 20 to 22.5 mm (2231), 22.5 to 25 mm (850), 25 to 27.5 mm (301) and >27.5 mm (126).

3.2 | Co-infections

Co-infections by two trematodes were far less common than expected by random chance (Fisher's exact test, $p < 0.001$; Figure 3). Co-infections by more than two taxa in a single snail were never observed. The four pairwise combinations that had the most negative difference between expected and observed co-infection frequencies were also the four pairwise combinations that showed the most evidence for negative interspecific interactions in the infection probability curves—that is a shift from monotonic increasing to unimodal at high prevalence of an abundant taxon. These combinations were *Metagonimus* sp. with three other taxa (*M. oregonensis*, *N. salmincola* and *A. oregonense*) and *N. salmincola* with *A. oregonense* (Figure 3, bottom combinations). All co-infection frequencies involving the two taxa showing monotonic increasing age-prevalence curves in the full dataset (*M. oregonensis* and *N. salmincola*) were less common than expected by chance (Figure 3). Only five of 28 combinations were equally or more common than expected, and these all involved at least one taxon with a unimodal age-prevalence curve.

3.3 | Age-prevalence models

The models demonstrated how parasite–parasite interactions, changes in the FOI and host mortality can each potentially affect age-prevalence curves. In the first scenario in the absence of other mechanisms, interactions between parasites alone were capable of generating a unimodal age-prevalence curve for the subordinate parasite (Figure 4a). The peak prevalence of the subordinate parasite occurred at an earlier age as the FOI of the dominant parasite increased (Figure 4a). In the second scenario where the FOI increased with host age for the dominant parasite, the peak prevalence of the subordinate parasite shifted to younger ages and the decline in older hosts became more rapid (Figure 4b). In the third scenario, infection-induced host mortality lowered the plateau of the curves for whichever taxa experienced greater mortality (Figure 4c). Mortality from infection that was constant over host age did not generate a unimodal curve in the dominant parasite but did shift the peak prevalence of the subordinate parasite towards a younger age (Figure 4c). The only mechanism that created a unimodal age-prevalence curve in the dominant parasite was the fourth scenario where infection-induced mortality
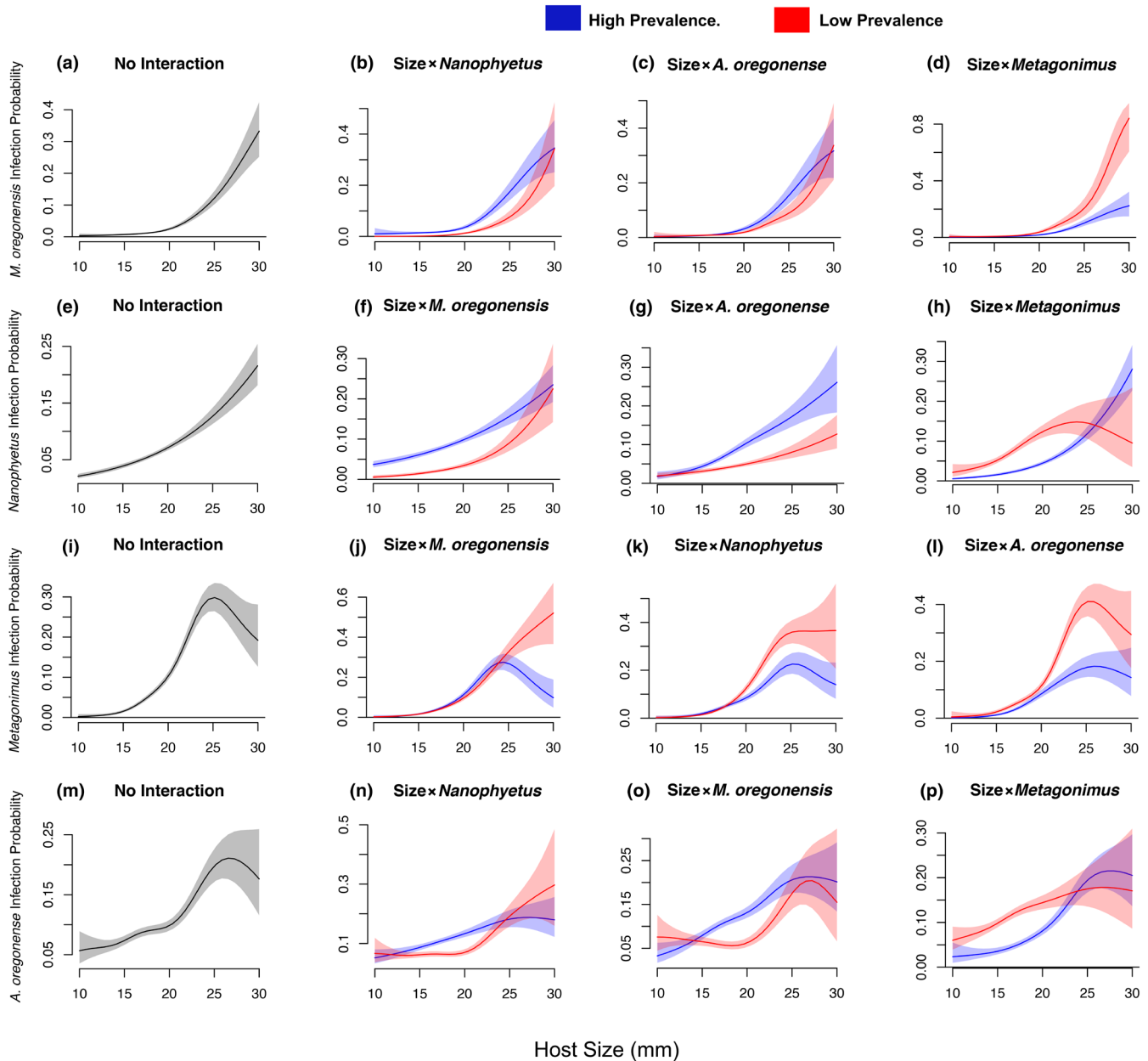
FIGURE 2 Partial effects plots for the effects of host size on infection probability of the four most abundant trematodes. The plots show results from a model with only host size (far left column), and models with interactions between host size and other potentially interacting trematodes. For models with interactions, the curve in blue reflects a high prevalence of the potentially interacting trematode and the curve in red reflects a low prevalence of the potentially interacting trematode. The identity of the focal trematode is shown on the *y*-axis label, and includes *M. oregonensis* (a, b, c, d), *N. salmincola* (e, f, g, h), *Metagonimus* sp. (i, j, k, l), and *A. oregonense* (m, n, o, p). The values have been transformed from the logit scale to indicate infection probabilities. The shaded areas are 95% confidence bands. Note differences in the *y*-axis scale between taxa. See Figures S3–S6 for similar panels for the other taxa.

increased with host age (Figure 4d); in all other scenarios the dominant parasite had a monotonically increasing age-prevalence curve. The steady-state solutions for the PDEs showed the same patterns as the ODEs for all four scenarios (Appendix S2, Figure S1).

4 | DISCUSSION

The shape of age-prevalence curves reflects ecological processes that underlie host–parasite interactions, including the

rates at which hosts gain, lose or are killed by infection (Heisey et al., 2006). Interactions between parasites have been posited as a contributing factor in shaping age-prevalence curves, but few studies have examined their roles in a multi-species parasite community. Here, we used an empirical dataset and models to demonstrate how parasite–parasite interactions can affect age-prevalence curves. Several lines of evidence suggest that parasite–parasite interactions were likely contributing to the unique distributions of the age-prevalence curves across parasite taxa in our dataset.
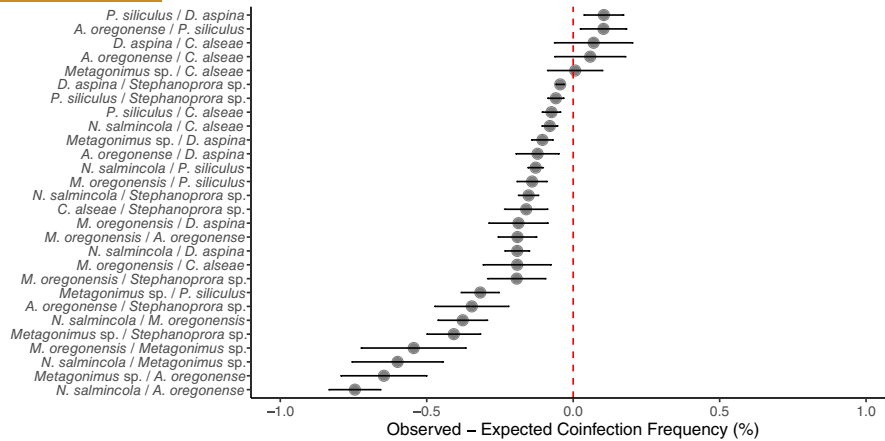
FIGURE 3 The observed minus expected frequency of co-infections between trematode taxa. Each combination of taxon identities is labelled on the left axis. Data are only from sites where the two taxa within each combination co-occurred. Values less than zero suggest negative interspecific interactions between parasites. Expected frequencies were calculated as the product of the two observed infection prevalences of the two taxa. Observed frequencies were those measured at each site based on dissections. Values are shown by their mean plus/minus one standard error. The vertical dashed line shows when the observed frequency equals the expected frequency.
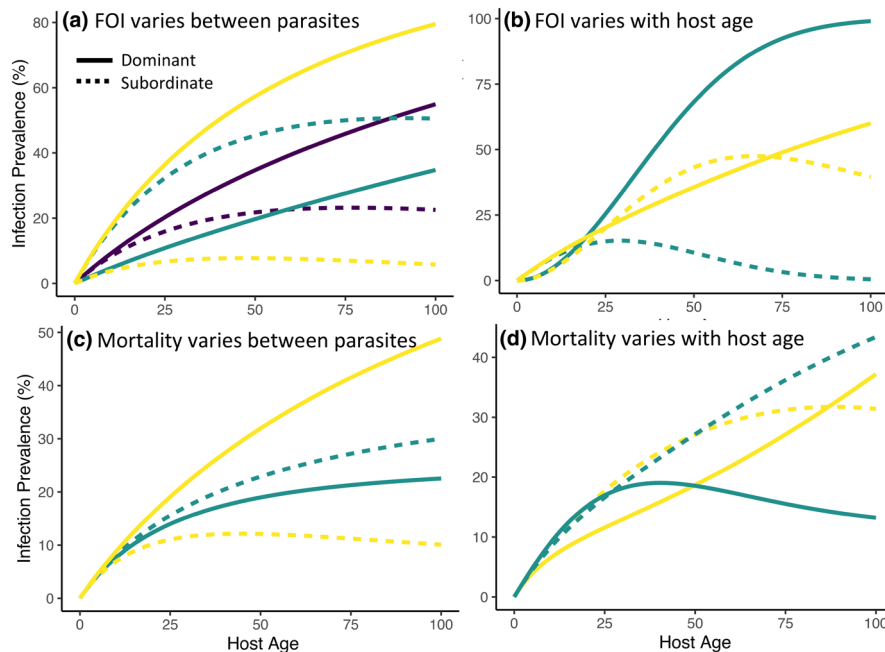

FIGURE 4 Results of ordinary differential equation analyses showing infection prevalence of a cohort of hosts over time that are infected with either a dominant parasite (solid line) or subordinate parasite (dashed line) for a given set of parameters (indicated by line colour, see Table 1 for specific parameter values). Panels corresponded to scenarios in which (a) the force-of-infection (FOI) is equal between the two parasites (purple lines), the FOI is higher for the subordinate (teal lines), or the FOI is higher for the dominant (yellow lines), all with constant mortality; (b) the FOI increases with host age for the dominant (teal lines), or the FOI increases with host age for the subordinate (yellow lines), all with constant mortality; (c) the infection-induced mortality rate is higher for the dominant (teal lines), or the infection-induced mortality rate is higher for the subordinate (yellow lines), all with a constant FOI; (d) the infection-induced mortality rate increases with host age for the dominant (teal lines), or the infection-induced mortality rate decreases with host age for the dominant (yellow lines), all with a constant FOI.

The empirical data across all survey sites showed that four taxa had monotonic increasing age-prevalence curves and four had unimodal curves. Monotonic increasing curves appear to be more common (about 70% of field studies; Sorensen &

Minchella, 2001) than unimodal curves in other snail-trematode systems (Esch & Fernandez, 1994; Snyder & Esch, 1993). The monotonic increasing infection prevalence of all taxa combined does not support the hypothesis that hosts are clearing their

infections at a high rate across all taxa, although we cannot rule out this mechanism entirely for individual taxa. Previous lines of evidence indicate trematode infections, once established in a host snail, may persist for the life of the host, particularly for long-lived snails (Kuris, 1990; Sousa, 1993). That said, a large body of research has characterized host snail immune responses to trematodes, which can lead to clearance of infections in some host–parasite combinations (Pila et al., 2017), but have not been quantified for most trematodes aside from those causing schistosomiasis in humans. Alternatively, if negative interspecific interactions between trematodes and variation in the FOI across taxa are underlying age-prevalence patterns in the field data, we would hypothesize that the taxa with monotonic increasing curves are competitively dominant to the taxa with unimodal curves. Several lines of evidence support this hypothesis, including the co-infection patterns.

The coinfection data supported the hypothesis that the trematodes with monotonic increasing curves were dominant to those with unimodal curves. For instance, the two most common taxa with monotonic increasing curves (*M. oregonensis* and *N. salmincola*) had large negative differences between their observed and expected co-infection frequencies, suggesting the presence of negative interspecific interactions. Two of the taxa with unimodal curves (*D. aspina* and *P. siliculus*) had co-infection frequencies that were relatively close to or more common than expected by chance, suggesting neutral or possibly positive interactions. These patterns, in part, aligned with expectations based on traits of the trematodes, including whether they possess a mouth (i.e. rediae stage) or do not (i.e. sporocyst stage). Prior studies have used morphological characteristics to hypothesize a dominance hierarchy (Kuris, 1990), typically assuming that trematodes with rediae stages are dominant to those with only sporocyst stages inside the snail (e.g. Alda et al., 2019; Soldánová et al., 2012). The trematode community in our study included five taxa with rediae and three with sporocysts (see Appendix S1, Table S3 for information on trematode life stages within snails and body size measurements of rediae or sporocysts). The two taxa that appear dominant both have rediae, although we note that some that appear most subordinate (e.g. *D. aspina*) also have rediae. The size of the pharynx has also been assumed to be correlated with dominance, but our results do not follow this assumption (e.g. *M. oregonensis*, a species with a small pharynx appeared dominant, while *D. aspina*, a species with a large pharynx, appeared subordinate). These results suggest that assuming a dominance hierarchy based on species traits may be challenging without other complimentary lines of evidence (Kuris, 1990).

Examining replicate age-prevalence curves over variation in the abundance of potentially interacting taxa provided support for the role of interspecific interactions in shaping the empirical curves for some, but not all, pairwise combinations. We hypothesized that subordinate trematodes would show a shift in their age-prevalence curves from unimodal to monotonic increasing when dominant taxa were at low abundance. Conversely, we expected that the curves of dominant taxa would remain monotonic increasing regardless of the prevalence of other taxa. Given these expectations, we interpreted several of the shifts in age-prevalence curves to be the result of negative interspecific interactions. Specifically, the age-prevalence curve of *Metagonimus* sp. shifted in the predicted way in relation to the prevalence of *M. oregonensis* and *N. salmincola*, which appear to be the competitively dominant taxa in the community. Similarly, *A. oregonense* (competitively inferior) showed the predicted shift in its curve in relation to *N. salmincola* (competitively dominant). These results are all consistent with observed co-infection frequencies among these taxa. The other taxa with unimodal curves were relatively rare, making it more challenging to detect shifts in their curves. The hypothesized dominant taxa (*M. oregonensis* and *N. salmincola*) had relatively consistent monotonic increasing age-prevalence curves in relation to most other taxa, consistent with predictions (although we do note variation in the slope that may be due to variation in the FOI over space). Interestingly, one dominant taxon (*N. salmincola*) had a unimodal curve with low prevalence of *Metagonimus* and a monotonic curve with high prevalence of *Metagonimus*. This pattern could possibly be due to some environmental variable being correlated with *Metagonimus* prevalence that also affected the shape of the curve for *N. salmincola*. Based on the co-infection data it seems unlikely that facilitation is occurring between these taxa in any way. Importantly, the analysis of age-prevalence curves from the survey data controlled for one interacting trematode at a time, and it is possible that shifts in the curves were obscured with this approach because the trematodes interacted with multiple other taxa concurrently at the host population scale (i.e. the curve for one trematode was affected by multiple other interacting trematode taxa). Incorporating the complexity of the multispecies setting, including potential indirect positive effects among directly competing taxa (Wootton, 1994) represents a useful next step for the modelling and empirical analysis of age-prevalence curves. Furthermore, our approach to analysing age-prevalence curves in the field data omitted other sources of unmeasured variation (e.g. possible changes in FOI over the life span of snails at the same site; Hudson & Dobson, 1995), making it especially notable that we were still able to detect some evidence of interspecific interactions.

The models helped clarify processes that can lead to unimodal age-prevalence curves and what causes the peak of the curve to shift. Unimodal age-prevalence curves are typically attributed to host mortality or clearance of infections in older hosts (Anderson & May, 1979; Esch & Fernandez, 1994). Host mortality, however, can only produce a unimodal curve when mortality increases with host age. In the models, the dominant parasite never showed a unimodal curve under any scenario with a constant infection-induced mortality rate, a finding described originally in models by Anderson and May (1979). In our model scenarios, the subordinate parasite almost always showed a unimodal age-prevalence curve, except when infection-induced mortality of the dominant parasite was high. The peak prevalence of the subordinate parasite shifted

to an earlier age as the FOI of the dominant parasite increased. Increasing host mortality caused by the subordinate parasite also shifted the peak prevalence to a younger age, and unlike the dominant parasite, this did not require mortality rates to increase with age. These patterns are similar to the peak shift in prevalence to younger hosts that has been observed when the FOI increases in hosts that acquire immunity to infection over time (Cattadori et al., 2005; Woolhouse, 1998). A peak shift due to acquired immunity has also been observed in experimental and field data on helminth infections in vertebrate definitive hosts, including rodents and humans (Crombie & Anderson, 1985; Fulford et al., 1992; Mutapi et al., 1997).

Variation in the FOI is an important factor shaping empirical age-prevalence curves. In the absence of other mechanisms, changes in the FOI should affect the steepness and plateau of the age-prevalence curve (Heisey et al., 2006) but should not cause changes from monotonic to unimodal. When interactions between parasites are considered, the peak prevalence of the subordinate parasite shifted to an earlier age as the FOI of the dominant parasite increased. We suspect this may be a common mechanism causing shifts in the peak prevalence of trematodes in snails and potentially other parasites that engage in negative interspecific interactions. We also incorporated an increasing FOI with host age/size into model scenarios as this has been observed in a variety of host–parasite interactions including trematode infections in snails (e.g. Daoust et al., 2010; Horn et al., 2023). However, in some snail-trematode interactions, host size may be positively correlated to exposure risk but negatively correlated to infection success by individual parasites (Shaw et al., 2022). More broadly across host–parasite systems, infection rates can be higher in younger, intermediate or older hosts (e.g. Theron & Rognon, 1998; Wunderlich et al., 2022), adding additional variation to age-prevalence curves that could be incorporated into models that capture system-specific attributes.

Analyses of age-intensity curves, which characterize changes in parasite numbers per host, show some similar patterns to our model and empirical data on age-prevalence curves. Analysing age-intensity curves is well-suited to host–parasite systems with traditional macroparasite life stages, such as helminth worms in second intermediate or definitive hosts that do not multiply within the host. For instance, Duerr et al. (2003) and Bottomley et al. (2005) used models to demonstrate how interspecific interactions between parasites affect parasite aggregation and can generate a wide array of saturating, unimodal or sigmoid age-intensity curves, depending on the underlying processes. In those modelling studies, negative interspecific interactions were able to generate unimodal age-intensity curves that were qualitatively similar to the age-prevalence curves reported in our study. Age-intensity curves have also been used to disentangle the potential roles of parasite clearance relative to host susceptibility (Park & Ezenwa, 2020), which may be more challenging to differentiate based on age-prevalence curves. Models that link individual level processes affecting infection intensity (e.g. immune responses)

to population level processes affecting prevalence (e.g. effects of infection on reproduction) would help merge perspectives on age-intensity and age-prevalence curves for systems where both measures are informative.

Moving forward, experimental approaches would be useful to directly test the role of parasite–parasite interactions in shaping age-prevalence curves. Tracking infected hosts over time in the field to quantify the rates at which infections are gained or lost would be useful in overcoming some of the limitations of observational field data (e.g. Buck et al., 2017). This type of approach would facilitate fitting FOI models to the empirical data and could more directly test whether and how parameters (e.g. infection rates, host mortality) vary with host age or other traits. Controlled exposures of snails to competing trematodes in the laboratory setting, although logistically challenging, could also directly test which species are competitively dominant and inferior to one another. Importantly, our modelling and observational results provide several lines of consistent evidence, but the complexity of multiple potentially synergistic underlying disease processes, as well as the multi-species nature of the parasite community, means our interpretations should be tempered by the need for further empirical studies. Lastly, it will also be useful to place the possible roles of interspecific interactions into the broader context of biotic and abiotic factors shaping community structure across space and time (Brian & Aldridge, 2021). While negative interspecific interactions are potentially important at the individual host scale, it is less clear to what degree they shape community structure of parasites at landscape (or watershed) scales.

AUTHOR CONTRIBUTIONS

Landon P. Falke and Daniel L. Preston conceived the survey design; Landon P. Falke led data collection; Mark Novak and Daniel L. Preston led modelling and statistical analyses; all authors contributed critically to the drafts and gave final approval for publication.

ACKNOWLEDGEMENTS

CONFLICT OF INTEREST STATEMENT

The authors declare no conflict of interest.

DATA AVAILABILITY STATEMENT

Data are available from the Dryad Digital Repository: https://doi.org/10.5061/dryad.x3ffbg7vf (Preston et al., 2024).

ORCID

Daniel L. Preston https://orcid.org/0000-0002-0486-3466

REFERENCES

Agresti, A. (2012). *Categorical data analysis*. New York, NY: John Wiley & Sons.

Alda, P., Bonel, N., Cazzaniga, N. J., Martorelli, S. R., & Lafferty, K. D. (2019). A strong colonizer rules the trematode guild in an intertidal snail host. *Ecology, 100*, e02696.

Anderson, R. M., & May, R. M. (1979). Prevalence of schistosome infections within molluscan populations: Observed patterns and theoretical predictions. *Parasitology, 79*, 63–94.

Anderson, R. M., & May, R. M. (1985). Herd immunity to helminth infection and implications for parasite control. *Nature, 315*, 493–496.

Bennington, E., & Pratt, I. (1960). The life history of the salmon-poisoning fluke, *Nanophyetus salmincola* (Chapin). *The Journal of Parasitology, 46*, 91–100.

Bottomley, C., Isham, V., & Basáñez, M.-G. (2005). Population biology of multispecies helminth infection: Interspecific interactions and parasite distribution. *Parasitology, 131*, 417–433.

Brian, J. I., & Aldridge, D. C. (2021). Abundance data applied to a novel model invertebrate host shed new light on parasite community assembly in nature. *Journal of Animal Ecology, 90*, 1096–1108.

Buck, J. C., Hechinger, R. F., Wood, A. C., Stewart, T. E., Kuris, A. M., & Lafferty, K. D. (2017). Host density increases parasite recruitment but decreases host risk in a snail-trematode system. *Ecology, 98*, 2029–2038.

Burnham, K. P., & Anderson, D. (2003). *Model selection and multi-model inference. A practical information theoretic approach*. Springer Verlag.

Burns, W. C. (1961). Six virgulate xiphidiocercariae from Oregon, including redescriptions of *Allassogonoporus vespertilionis* and *Acanthatrium oregonense*. *The Journal of Parasitology, 47*, 919–925.

Burns, W. C., & Pratt, I. (1953). The life cycle of *Metagonimoides oregonensis* Price (Trematoda: Heterophyidae). *The Journal of Parasitology, 39*, 60–69.

Byers, J. E., Malek, A. J., Quevillon, L. E., Altman, I., & Keogh, C. L. (2015). Opposing selective pressures decouple pattern and process of parasitic infection over small spatial scale. *Oikos, 124*, 1511–1519.

Caley, P., & Hone, J. (2002). Estimating the force of infection; *Mycobacterium bovis* infection in feral ferrets *Mustela furo* in New Zealand. *Journal of Animal Ecology, 71*, 44–54.

Caley, P., Marion, G., & Hutchings, M. R. (2009). Assessment of transmission rates and routes, and the implications for management. In R. J. Delahay, G. C. Smith, & M. R. Hutchings (Eds.), *Management of disease in wild mammals* (pp. 31–51). Springer Verlag.

Campbell, D. C., Clark, S. A., Johannes, E. J., Lydeard, C., & Frest, T. J. (2016). Molecular phylogenetics of the freshwater gastropod genus *Juga* (Cerithioidea: Semisulcospiridae). *Biochemical Systematics and Ecology, 65*, 158–170.

Cattadori, I. M., Boag, B., Bjørnstad, O. N., Cornell, S. J., & Hudson, P. J. (2005). Peak shift and epidemiology in a seasonal host–nematode system. *Proceedings of the Royal Society B: Biological Sciences, 272*, 1163–1169.

Cattadori, I. M., Boag, B., & Hudson, P. J. (2008). Parasite co-infection and interaction as drivers of host heterogeneity. *International Journal for Parasitology, 38*, 371–380.

Cohen, J. E. (1973). Selective host mortality in a catalytic model applied to schistosomiasis. *The American Naturalist, 107*, 199–212.

Crombie, J. A., & Anderson, R. M. (1985). Population dynamics of *Schistosoma mansoni* in mice repeatedly exposed to infection. *Nature, 315*, 491–493.

Daoust, S. P., Mader, B. J., Maure, F., McLaughlin, J. D., Thomas, F., & Rau, M. E. (2010). Experimental evidence of size/age-biased infection of *Biomphalaria glabrata* (Pulmonata: Planorbidae) by an incompatible parasite species: Consequences for biological control. *Infection, Genetics and Evolution, 10*, 1008–1012.

Diamond, J. M. (1982). Stream geomorphology and benthic habitat predictability as determinants of the population dynamics and life history of the snail *Juga plicifera*. *Journal of Freshwater Ecology, 1*, 577–588.

Dueger, E. L., & Gilman, R. H. (2001). Prevalence, intensity, and fertility of ovine cystic echinococcosis in the central Peruvian Andes. *Transactions of the Royal Society of Tropical Medicine and Hygiene, 95*, 379–383.

Duerr, H. P., Dietz, K., & Eichner, M. (2003). On the interpretation of age–intensity profiles and dispersion patterns in parasitological surveys. *Parasitology, 126*, 87–101.

Esch, G. W., & Fernandez, J. C. (1994). Snail-trematode interactions and parasite community dynamics in aquatic systems: A review. *American Midland Naturalist, 131*, 209–237.

Ezenwa, V. O. (2016). Helminth–microparasite co-infection in wildlife: Lessons from ruminants, rodents and rabbits. *Parasite Immunology, 38*, 527–534.

Falke, L. P., & Preston, D. L. (2021). Infection prevalence and density of a pathogenic trematode parasite decrease with stream order along a river continuum. *Ecosphere, 12*, e03670.

Falke, L. P., & Preston, D. L. (2022). Freshwater disease hotspots: Drivers of fine-scale spatial heterogeneity in trematode parasitism in streams. *Freshwater Biology, 67*, 487–497.

Fenton, A. (2008). Worms and germs: The population dynamic consequences of microparasite-macroparasite co-infection. *Parasitology, 135*, 1545–1560.

Fulford, A. J. C., Butterworth, A. E., Sturrock, R. F., & Ouma, J. H. (1992). On the use of age-intensity data to detect immunity to parasitic infections, with special reference to *Schistosoma mansoni* in Kenya. *Parasitology, 105*, 219–227.

Graham, A. L. (2003). Effects of snail size and age on the prevalence and intensity of avian schistosome infection: Relating laboratory to field studies. *Journal of Parasitology, 89*, 458–463.

Hairston, N. G. (1965). An analysis of age-prevalence data by catalytic models: A contribution to the study of bilharziasis. *Bulletin of the World Health Organization, 33*, 163–175.

Halliday, F. W., Penczykowski, R. M., Barrès, B., Eck, J. L., Numminen, E., & Laine, A.-L. (2020). Facilitative priority effects drive parasite assembly under coinfection. *Nature Ecology & Evolution, 4*, 1510–1521.

Hawkins, C. P., & Furnish, J. K. (1987). Are snails important competitors in stream ecosystems? *Oikos, 49*, 209–220.

Hechinger, R. F., Wood, A. C., & Kuris, A. M. (2011). Social organization in a flatworm: Trematode parasites form soldier and reproductive castes. *Proceedings of the Royal Society B: Biological Sciences, 278*, 656–665.

Heisey, D. M., Joly, D. O., & Messier, F. (2006). The fitting of general force-of-infection models to wildlife disease prevalence data. *Ecology, 87*, 2356–2365.

Heyneman, D., & Umathevy, T. (1968). Interaction of trematodes by predation within natural double infections in the host snail *Indoplanorbis exustus*. *Nature, 217*, 283–285.

Horn, C. J., Liang, C., & Luong, L. T. (2023). Parasite preferences for large host body size can drive overdispersion in a fly-mite association. *International Journal for Parasitology, 53*, 327–332.

Hudson, P. J., & Dobson, A. P. (1995). Macroparasites: Observed patterns in naturally fluctuating animal populations. In B. T. Grenfell, A. P. Dobson, & A. P. Dobson (Eds.), *Ecology of infectious diseases in natural populations* (pp. 144–176). Cambridge University Press.

Johnson, P. T., & Hoverman, J. T. (2012). Parasite diversity and coinfection determine pathogen infection success and host fitness. *Proceedings of the National Academy of Sciences of the United States of America, 109*, 9006–9011.

Karvonen, A., Jokela, J., & Laine, A.-L. (2019). Importance of sequence and timing in parasite coinfections. *Trends in Parasitology, 35*, 109–118.

Kuris, A. (1990). Guild structure of larval trematodes in molluscan hosts: Prevalence, dominance and significance of competition. In G. W. Esch, A. O. Bush, & J. M. Aho (Eds.), *Parasite communities: Patterns and processes* (pp. 69–100). Chapman and Hall.

Lafferty, K. D. (2002). Interspecific interactions in trematode communities. In E. E. Lewis, J. F. Campbell, & M. V. Sukhdeo (Eds.), *The behavioural ecology of parasites* (pp. 153–170). CABI Publishing.

Lie, K. J. (1973). Larval trematode antagonism: Principles and possible application as a control method. *Experimental Parasitology, 33*, 343–349.

Lim, H.-K., & Heyneman, D. (1972). Intramolluscan inter-trematode antagonism: A review of factors influencing the host–parasite system and its possible role in biological control. *Advances in Parasitology, 10*, 191–268.

Marchetto, K. M., & Power, A. G. (2018). Coinfection timing drives host population dynamics through changes in virulence. *The American Naturalist, 191*, 173–183.

McCallum, H., Barlow, N., & Hone, J. (2001). How should pathogen transmission be modelled? *Trends in Ecology & Evolution, 16*, 295–300.

McCauley, J. E., & Pratt, I. (1961). A new genus *Deropegus* with a redescription of *D. aspina* (Ingles, 1936) nov. comb. *Transactions of the American Microscopical Society, 80*, 373–377.

Meade, T. G., & Pratt, I. (1965). Description and life history of *Cardicola alseae* sp. n. (Trematoda: Sanguinicolidae). *The Journal of Parasitology, 51*, 575–578.

Muench, H. (1959). *Catalytic models in epidemiology.* Harvard University Press.

Mutapi, F., Ndhlovu, P. D., Hagan, P., & Woolhouse, M. E. J. (1997). A comparison of humoral responses to *Schistosoma haematobium* in areas with low and high levels of infection. *Parasite Immunology, 19*, 255–263.

Park, A. W., & Ezenwa, V. O. (2020). Characterising interactions between co-infecting parasites using age-intensity profiles. *International Journal for Parasitology, 50*, 23–26.

Pedersen, A. B., & Fenton, A. (2007). Emphasizing the ecology in parasite community ecology. *Trends in Ecology & Evolution, 22*, 133–139.

Petney, T. N., & Andrews, R. H. (1998). Multiparasite communities in animals and humans: Frequency, structure and pathogenic significance. *International Journal for Parasitology, 28*, 377–393.

Pila, E. A., Li, H., Hambrook, J. R., Wu, X., & Hanington, P. C. (2017). Schistosomiasis from a snail's perspective: Advances in snail immunity. *Trends in Parasitology, 33*, 845–857.

Poulin, R. (2000). Variation in the intraspecific relationship between fish length and intensity of parasitic infection: Biological and statistical causes. *Journal of Fish Biology, 56*, 123–137.

Pratt, I., & McCauley, J. E. (1961). *Trematodes of the Pacific Northwest. An annotated catalog.* Oregon State University Press.

Preston, D. L., Falke, L. P., & Novak, M. (2024). Data from: Age-prevalence curves in a multi-species parasite communities [Data set]. *Dryad Digital Repository.* https://doi.org/10.5061/dryad.x3ffbg7vf

Preston, D. L., Layden, T. J., Segui, L. M., Falke, L. P., Brant, S. V., & Novak, M. (2021). Trematode parasites exceed aquatic insect biomass in Oregon stream food webs. *Journal of Animal Ecology, 90*, 766–775.

R Core Team. (2023). *R: A language and environment for statistical computing.* Vienna, Austria: R Foundation for Statistical Computing. https://www.R-project.org/

Rynkiewicz, E. C., Pedersen, A. B., & Fenton, A. (2015). An ecosystem approach to understanding and managing within-host parasite community dynamics. *Trends in Parasitology, 31*, 212–221.

Shaw, K. E., Cloud, R. E., Syed, R., & Civitello, D. J. (2024). Parasite transmission in size-structured populations. *Ecology, 105*(2), e4221.

Smith, N. F. (2001). Spatial heterogeneity in recruitment of larval trematodes to snail intermediate hosts. *Oecologia, 127*, 115–122.

Snyder, S. D., & Esch, G. W. (1993). Trematode community structure in the pulmonate snail Physa gyrina. *The Journal of parasitology*, 205–215.

Soetaert, K., Petzoldt, T., & Setzer, R. W. (2010). Solving differential equations in R: Package deSolve. *Journal of Statistical Software, 33*, 1–25.

Soldánová, M., Kuris, A. M., Scholz, T., & Lafferty, K. D. (2012). The role of spatial and temporal heterogeneity and competition in structuring trematode communities in the great pond snail, *Lymnaea stagnalis* (L.). *Journal of Parasitology, 98*, 460–471.

Sorensen, R. E., & Minchella, D. J. (2001). Snail–trematode life history interactions: Past trends and future directions. *Parasitology, 123*, S3–S18.

Sousa, W. P. (1993). Interspecific antagonism and species coexistence in a diverse guild of larval trematode parasites. *Ecological Monographs, 63*, 103–128.

Strong, E. E., & Whelan, N. V. (2019). Assessing the diversity of Western North American *Juga* (Semisulcospiridae, Gastropoda). *Molecular Phylogenetics and Evolution, 136*, 87–103.

Susi, H., Barrès, B., Vale, P. F., & Laine, A.-L. (2015). Co-infection alters population dynamics of infectious disease. *Nature Communications, 6*, 5975.

Theron, A., & Rognon, A. (1998). Host choice by larval parasites: A study of *Biomphalaria glabrata* snails and *Schistosoma mansoni* miracidia related to host size. *Parasitology Research, 84*, 727–732.

Viney, M. E., & Graham, A. L. (2013). Patterns and processes in parasite co-infection. *Advances in Parasitology, 82*, 321–369.

Wilson, E. B. (1927). Probable inference, the law of succession, and statistical inference. *Journal of the American Statistical Association, 22*, 209–212.

Wood, S. N. (2017). *Generalized additive models: An introduction with R.* CRC press.

Woolhouse, M. E. J. (1998). Patterns in parasite epidemiology: The peak shift. *Parasitology Today, 14*, 428–434.

Woolhouse, M. E. J., Bealby, K., McNamara, J. J., & Silutongwe, J. (1994). Trypanosome infections of the tsetse fly *Glossina pallidipes* in the Luangwa Valley, Zambia. *International Journal for Parasitology, 24*, 987–993.

Wootton, J. T. (1994). The nature and consequences of indirect effects in ecological communities. *Annual Review of Ecology and Systematics, 25*, 443–466.

Wunderlich, A., Simioni, W., Zica, É., & Siqueira, T. (2022). Experimental evidence that host choice by parasites is age-dependent in a fish-monogenean system. *Parasitology Research, 121*, 115–126.

SUPPORTING INFORMATION

Additional supporting information can be found online in the Supporting Information section at the end of this article.

Appendix S1. Supporting statistical results and study area map.

Appendix S2. Details on partial differential equations.